Chapter 8
Applications of Acousto-Optics

8.1 INTRODUCTION

Most applications of acousto-optics utilize the two important characteristics of the interaction:

1. The angle of the deflected beam is roughly proportional to the acoustic frequency;
2. The frequency information in the acoustic wave is impressed onto the diffracted optic beam.

Devices range from the relatively mature beam deflecters operating at low frequencies and using isotropic glasses to the more sophisticated wideband or high resolution spectrum analyzers. The latter devices, which are our main concern, involve acoustic techniques and interaction geometries, which require a complete understanding of all aspects of the A/O interaction. It should not be surprising that they are both difficult and costly to fabricate.

In this chapter, we examine A/O devices, emphasizing the influence of acoustic techniques. In this respect, our study is far from complete, but is intended to illustrate practical applications of wideband acoustic theory and to introduce some practical and interesting devices. The performance of these devices is characterized by the power (RF) required to deflect a given light intensity, the device bandwidth, and the number of resolvable deflected optic beams. Depending on the particular application, usually only one or two of these factors is critical to the overall device performance. This is fortunate because theoretical and fabrication limitations impose trade-offs in the design of commercial devices, making it difficult to optimize all these factors simultaneously. There are performance enhancements that dramatically increase one or more of these characteristics. We do not calculate the photoelastic constant in this discussion, and thus we

cannot determine the intensity of the diffracted optical beam. This calculation is performed in Chapter 9, when we investigate the structure of the A/O interaction. The theory developed there completes the description of the interaction.

8.2 EFFICIENCY

Acousto-optic efficiency refers to the magnitude of the ratio of *diffracted* intensities to incident optic intensities for a given RF power. It is expressed as percent (of diffracted light) per watt (of RF) power. For laser beam deflectors and modulators that require that nearly all the incident light be coupled into the deflected beam, high A/O efficiency reduces the required RF drive and acoustic power (and therefore the heat loss). For spectrum analyzers in which only a small amount of light is diffracted, high efficiency reduces spurious responses in the RF amplifiers (caused by overdriving them) and nonlinear acoustic responses.

Equation (7.92) expresses the relation between the diffracted light intensity and acoustic intensity. To express the diffracted light as a linear function of acoustic power, we consider the region in which the diffracted light is small, and we make the approximation:

$$\sin^2(A) = A^2$$

Equation (7.92) becomes

$$\frac{I_d}{I_i} = \frac{\pi^2 x^2}{2\lambda_0^2}[M]I_a \tag{8.1}$$

where I_a is the acoustic intensity in W/m^2 and x is the interaction length. Even though (8.1) is valid only for low diffracted intensity, it does provide a convenient measure of device performance. Recall that the $\sin^2$ dependence in (7.92) is a consequence of the coupled equations ((7.81) and (7.82)) and results in the dynamic situation in which power is continuously being coupled either into or out of the diffracted beam. In a practical device, the acoustic beam has finite dimension, as shown in Figure 8.1, and the acoustic power is given by

$$P_a = I_a(LH) \tag{8.2}$$

where L is the length and H is the height of the acoustic transducer, which determine the dimension of the acoustic beam, and P_a is the acoustic power in watts. The interaction length is simply L, and (8.1) becomes

$$\frac{I_d}{I_i} = \frac{\pi^2 L}{2\lambda_0^2 H}[M]P_a \tag{8.3}$$

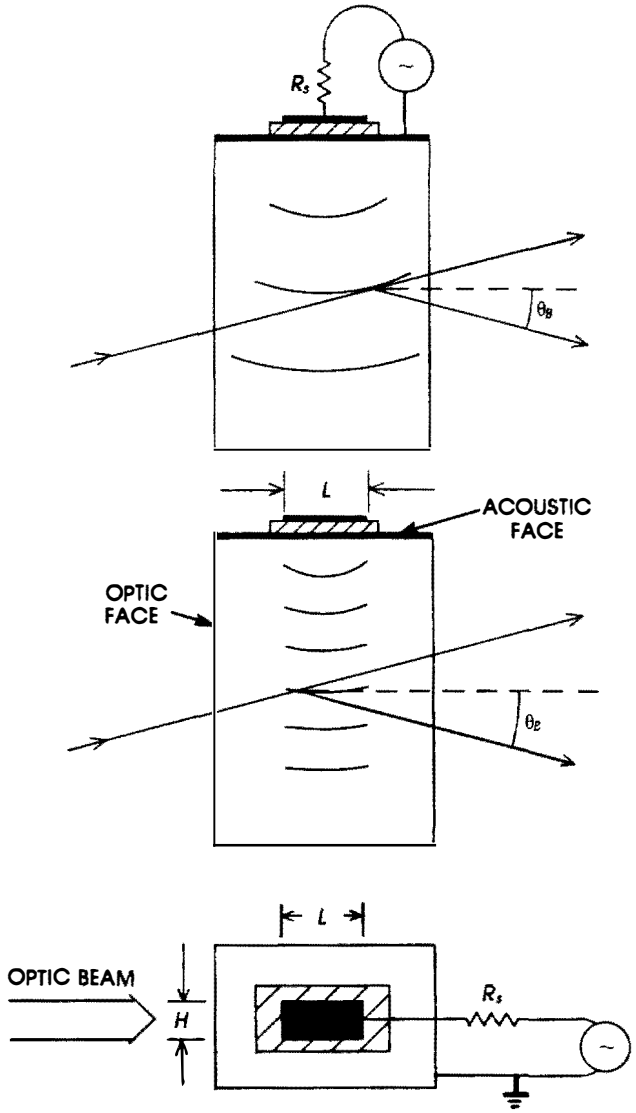

Figure 8.1 Schematic diagram showing the dimensions of the acoustic transducer as they relate to the optic beam.

Equation (8.3) assumes that the beam length L is constant over the optic aperture (see Figure 8.1) and that the interaction is uniform over L. Because both assumptions are usually grossly inaccurate, the results of (8.3) should be used with caution. At any rate, a diffracted beam intensity requires high acoustic power (P_a), a long (transducer) interaction length L, and small transducer height (H). Decreasing H, for example, results in greater acoustic and optic beam intensities if the optic beam is focused sufficiently so as to fill the acoustic beam completely (Figure 8.1). Because the efficiency is proportional to the interaction length, it is desirable to design the transducer with large L. Other factors, however, such as the device radiation resistance (which is inversely proportional to the device transducer area LH) and the Bragg bandwidth (which we consider in the next section), constrain the interaction length.

The figure of merit (FOM) for an A/O device acting as a beam deflector is M_2 and is derived in (7.94):

$$M_2 = \frac{n^6 p^2}{\rho v_a^3}$$

Of the factors that determine M_2, ρ is independent of the crystal orientation and optic wavelength (it varies only slightly with temperature), n depends on the optic mode (for a birefringent medium) and the optic wavelength, and v_a is determined from the Christoffel equation. The photoelastic constant refers to the effective p component and depends on the interaction geometry. We determine this constant in Chapter 9. Thus, in this chapter, we will not be able to determine the value of the intensity I_d. Instead, we will confine ourselves to finding the bandwidth.

Finally, (8.3) does not consider the conversion of RF power into acoustic energy. This factor depends on the transducer piezoelectric response, the ground plane metalization, and the quality of fabrication technology. In most devices, the RF to acoustic conversion results in a loss of 4 to 10 dB, although conversion losses less than 2 dB have been reported. Attaining high efficiency involves not only choosing materials with optimal A/O characteristics but also paying careful attention to acoustic techniques.

8.3 BANDWIDTH

If the transducer has an extremely large L, the interaction efficiency could be quite high but the acoustic beam would be nearly perfectly collimated. For a given optic wavelength, the Bragg condition (7.98) would be satisfied only for a very small band of acoustic frequencies, and the

Bragg bandwidth would be essentially nil. As a spectrum analyzer, modulator, or laser beam deflector, such a device clearly would be useless. A consequence of diffraction is that, as the frequency is varied, different regions of the acoustic beam satisfy the Bragg condition, as shown in Figure 8.2. As L decreases, the diffraction spread becomes greater, thus increasing the bandwidth. A smaller L, however, results in decreased diffraction efficiency. Also, as the bandwidth increases, a progressively smaller portion of the acoustic wave actually participates in the interaction process, thus further decreasing the diffracted light intensity and calling (8.3) into doubt.

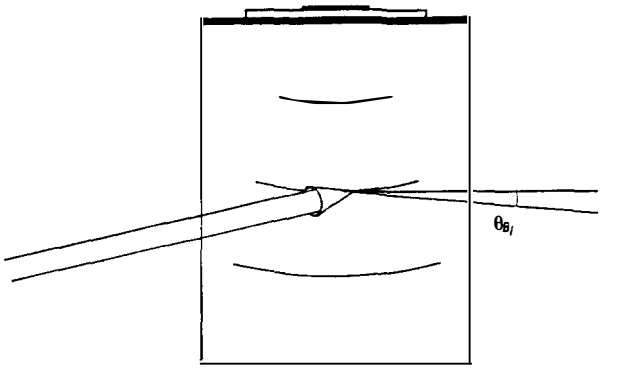

(a) LOW FREQUENCIES

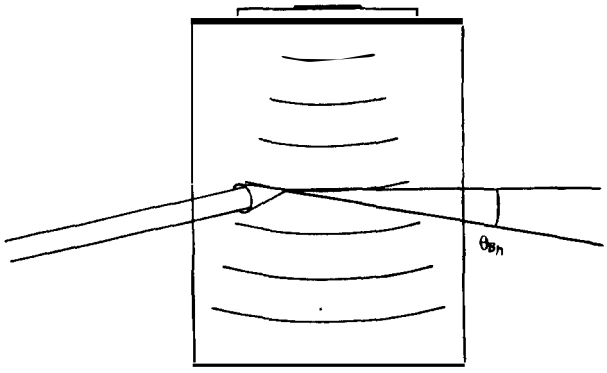

(b) HIGH FREQUENCIES

Figure 8.2 Bragg bandwidth in an isotropic interaction is a result of the diffraction spread of the acoustic wave: (a) at low frequencies the beam interacts on the right part, where it makes a small Bragg angle; (b) at high frequencies, the beam interacts on the left part.

To express the diffraction bandwidth formally, we return to the Bragg condition (isotropic),

$$\sin\theta_B = \frac{\lambda_0 f_s}{2v_a n} \tag{8.4}$$

where θ_B is the internal Bragg angle. Differentiating (8.4) with respect to frequency, we have

$$d\theta_B = \frac{\lambda_0 df_s}{2nv_a \cos\theta_B} \tag{8.5}$$

From elementary diffraction theory, the relation between the radiator dimension and the diffraction angle of the beam is

$$d\theta \sim \frac{\lambda_s}{L} = \frac{v_a}{Lf_s} \tag{8.6}$$

Substituting (8.6) into (8.5) and solving for df_s, we obtain

$$df_s = \frac{2nv_a^2 \cos\theta_B}{L\lambda_0 f_s} \tag{8.7}$$

A somewhat more sophisticated analysis gives the widely accepted formula for the bandwidth, which replaces the 2 by 1.8:

$$\text{BW} = \frac{1.8nv_a^2 \cos\theta_B}{L\lambda_0 f_s} \tag{8.8}$$

To attain wideband devices we require:

1. Use of materials with high refractive index and operation at short laser wavelengths. These conditions are identical to the requirements for high diffraction efficiency, but, as we previously mentioned, materials with high index usually cut off their light transmission near 1 μm.
2. Use of materials and crystal cuts with high acoustic velocity (longitudinal modes) that operate at low center frequencies and small transducer lengths. These requirements, which relate to the diffraction spread in the acoustic beam, conflict with the conditions for high efficiency (except for the condition of low center frequency). Because the efficiency is proportional to L/H, it is possible to achieve high efficiency and large bandwidth

by using an L that satisfies the bandwidth requirement and by reducing H until the device operates with the desired efficiency. Notice that (8.8) is independent of the photoelastic constant.

The overall device bandwidth is the product of the Bragg and *acoustic* bandwidths. Device design requires careful attention to transducer coupling constants, ground plane metalization, and thickness and impedance-matching considerations. To a reasonable approximation, the acoustic bandwidth is given by (5.63)

$$\Delta f = \text{BW} \approx \frac{4k_t^2}{\pi}\left[\frac{Z_S}{Z_T}\right] f_0 = Kf_0 \tag{8.9}$$

where K is a constant and f_0 is the center frequency. For a lithium niobate 36° $\langle y \rangle$-cut (assuming that the impedance mismatch is reasonable), (5.63) yields

$$\text{BW} = .3f_0 \tag{8.10}$$

The coupling constant for 36° $\langle y \rangle$ lithium niobate is less than the highest constant presently achievable (for $\langle x \rangle$ shear mode lithium niobate) but significantly higher than other possible piezoelectric transducers, such as quartz or zinc oxide. With careful attention to RF techniques, it is possible to achieve acoustic bandwidths greater than 50% by using this cut. Whatever the factor, (8.10) shows that the acoustic bandwidth is directly proportional to the center frequency.

Comparing (8.10) with (8.8) highlights the bandwidth design tradeoffs. At low acoustic frequencies, the bandwidth is limited by (8.10) because the beam will generally be uncollimated, resulting in large Bragg bandwidths. At high frequencies, the acoustic bandwidth remains between 20 to 70% of f_0, but the Bragg bandwidth becomes the limiting factor, because the required transducer length L for reasonably wide bandwidths may be so small that the device becomes quite difficult to fabricate. An additional consideration is the transducer clamped capacitance, which increases at high frequencies (because the thickness decreases), so matching techniques are required, which may limit the fractional acoustic bandwidth to less than 50%. At operating frequencies above 1 GHz, the dominant factor, however, is usually the difficulty of maintaining the required Bragg bandwidth. To emphasize the importance of wide bandwidth, we define a second FOM M_1:

$$M_1 = M_2(\mathrm{v}_a^2 n) \tag{8.11}$$

Example 8.1. We calculate the acoustic and Bragg bandwidths and radiation resistance for a longitudinal mode A/O deflector on ⟨1, 1, 0⟩ gallium phosphide operating in conjunction with a 36° ⟨*y*⟩ lithium niobate transducer in various frequency ranges. The optic wavelength is .83 μm (laser diode), and we assume the $L/H = 2$. For the substrate, $n = 3.3$ and $v_a = 6.3 \times 10^3$ m/s. For the transducers, $v_a = 7.4 \times 10^3$ m/s, $\epsilon_r = 35$, and $k_t^2 = .25$.

1. $f_0 = 100$ MHz and $L = 2$ mm

acoustic BW $\approx$ 50 MHz

$$\text{Bragg BW} = \frac{1.8nv_a^2}{L\lambda f_s} = 1.4 \times 10^9$$

$$R_a = \frac{4k_t^2}{\pi\omega_0 C_0} = 30\ \Omega$$

In this case, the bandwidth of the device is acoustically limited. Even though the fractional acoustic bandwidth is quite large in absolute terms, it is much less than the Bragg bandwidth, which is increased not only by the low center frequency but also by the high index of GaP and the relatively high velocity. Clearly, the acoustic transducer length could be dramatically increased before reaching Bragg limitations. Doing so, however, would make the device unwieldy and cause difficulty in matching, which would further reduce the acoustic bandwidth.

2. $f_0 = 2$ GHz and $L = .2$ mm (8 mils)

acoustic BW $= .5f_0 = 1$ GHz
Bragg BW $= .71$ GHz
$R_a = 6.3\ \Omega$

In this case, the bandwidths are relatively well matched. There is a potential problem due to the relatively low radiation resistance. Matching the device to 50 Ω may cause a slight reduction in the acoustic bandwidth, which is nevertheless quite substantial. This particular configuration of transducer and substrate is well suited to high performance A/O devices operating in the 2-GHz frequency range.

3. $f_0 = 3$ GHz and $L = .1$ mm (4 mils)

acoustic BW $= 1.5$ GHz
Bragg BW $= .91$ GHz
$R_a = 8.5\ \Omega$

In the high frequency case, the device is Bragg limited even though the transducer length is quite small. Decreasing L much further would cause difficulty with device fabrication and would introduce possible nonlinear spurious responses because of the high acoustic intensities. Because $L/H = 2$, the radiating area is 5×10^{-9} m^2. For an acoustic power of 1 W, the intensity is then 2×10^8 W/m^2! It is not surprising that acoustic nonlinearities are a problem, especially at high frequencies.

At frequencies above 2 GHz, the acoustic beam is so collimated that isotropic interactions become impractical. There are, however, techniques that increase the Bragg bandwidth at these frequencies without significantly sacrificing efficiency or resolution. As we remarked earlier, the bandwidth of birefringent interaction devices is not given by (8.8). As shown in Figure 7.9 for frequencies close to f_s' (the critical frequency), the deflected angle increases linearly with frequency even though the incident angle is stationary. Thus, in this region the acoustic beam can be completely collimated, and the deflected light angle will nevertheless vary linearly with frequency. Unfortunately, the frequency region in which the incident angle is stationary is quite limited, so L cannot be increased indefinitely. Later, we will examine quantitatively the bandwidth improvement.

8.4 RESOLUTION

Resolution, which refers to the achievable number of resolvable frequencies, is an important consideration in applications requiring the A/O interaction to decompose an RF band into its constituent frequencies by mapping the individual frequencies spatially. Examples are electronic intelligence, radio astronomy, and, to a lesser degree, electronic warfare (EW). As a practical matter, peripheral devices, such as photodetector arrays and postprocessing electronics, usually limit ultimate system performance. The number of resolvable frequencies or spatial "spots" is defined as

$$N = \frac{\Delta\theta_B}{\Delta\phi} \tag{8.12}$$

where $\Delta\phi$ is the diffraction spread in the optic beam and $\Delta\theta$ is the change in Bragg deflection angle as a function of acoustic frequency. We write (8.12) without the refractive index (because the frequencies are "resolved" outside the crystal):

$$\Delta\theta_B = \frac{\lambda_0}{v_a \cos\theta_B} \Delta f_s \tag{8.13}$$

and

$$\Delta\phi = \frac{\lambda_0}{D} \tag{8.14}$$

where D is the width of the optic beam, as shown in Figure 8.3. Substituting (8.13) and (8.14) into (8.12), we obtain

$$N = \left(\frac{D}{v_a \cos\theta_B}\right) \Delta f_s \tag{8.15}$$

The term in parentheses is the time required for the acoustic beam propagating with phase velocity v_a to traverse the optic beam of width D. We call this term τ, and we write

$$N = \tau \Delta f_s = \tau \, \mathrm{BW} \tag{8.16}$$

where BW is the overall bandwidth of the device. The quantity τBW is called the *time-bandwidth* product of the device.

In the interaction geometry of an A/O device optimized for high resolution, the critical factors are bandwidth and τ rather than efficiency. Such devices require use of crystal cuts with low acoustic velocity (usually shear modes), low acoustic attenuation, and *large* values of H. The latter requirement follows from the inverse relation of H to acoustic diffraction in the plane parallel to the optic beam. Further, the requirements of low velocity, low attenuation, and high bandwidth are usually not compatible. Thus, high resolution devices are forced to operate in regions of moderate center frequencies and bandwidth. For high resolution applications, a third FOM M_3 is defined as

$$M_3 = \frac{M_1}{v_a} \tag{8.17}$$

Example 8.2. Consider the slow shear mode in paratellurite (TeO_2). Because the acoustic velocity is $.62 \times 10^3$ m/s, an interaction length of 6.2 cm provides a τ of 100 μs (from (8.15)). Because the acoustic attenuation and diffraction losses are extremely high, the device is forced to operate

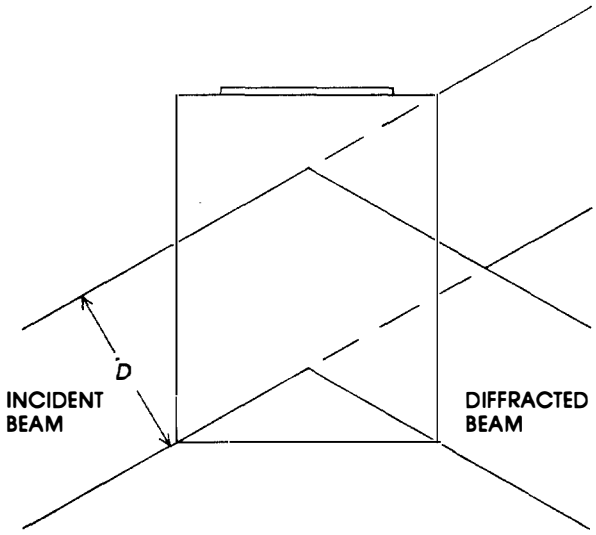

Figure 8.3 Interaction geometry for a high resolution application. The overlap between the optic and acoustic beam defines the optic aperture D.

at $f_0 = 100$ MHz, with a bandwidth of approximately 50 MHz. The number of resolvable spots is thus

$$N = \tau BW = 100\ \mu s \times 50 \times 10^6 = 5000$$

This is the number of positions that can be addressed simultaneously. Although these parameters are quite optimistic, such devices have been fabricated. Certainly no other technology can approach this performance.

8.5 ACOUSTO-OPTIC DEVICES

8.5.1 Beam Deflectors

The angular dependence of the diffracted light beam with frequency is employed to deflect a laser beam to a desired position. A beam may be continuously deflected by varying the frequency through a prescribed band. These devices require high deflection efficiency (because only the deflected beam is useful) and large time apertures (because precise control of the

laser beam is critical). Bandwidth requirements, however, are usually low to moderate. Typically, they are used to deflect either 1.06-μm radiation (Nd: YAG laser) or 10.6-μm radiation (CO_2 laser). Because the efficiency varies inversely with λ_0^{-2}, the interaction length L and RF power must be increased dramatically, especially at 10.6 μm. CO_2 deflectors require interaction crystals with very high M_2. Germanium (Ge) is a popular choice because its growth technology is quite mature, it transmits optical radiation well into the infrared (IR) region (its lower cutoff is about 2 μm), and it is readily available in large sizes. For a Ge deflector at 10.6 μm operating at a center frequency of 30 MHz (with a 10-MHz bandwidth), the transducer dimensions would typically be 15 × mm (L) × 3 mm (H). the radiation resistance is (for a longitudinal $LiNbO_3$ transducer):

$$C_0 = 3.5 \times 10^{-10} f \text{ and } \hat{R}_a \approx 10\ \Omega$$

Even though the radiation resistance is quite low (the area of the transducer is huge), the 30% bandwidth is relatively easy to achieve. The Bragg bandwidth (8.8) is greater than 30 MHz, which implies that L could be doubled (the device is acoustically limited). Increasing L would reduce $\hat{R}_a$ and increase the difficulty of electrical matching. Decreasing the transducer height would cause severe diffraction loss in the acoustic beam and decrease the time aperture τ.

At 1.06 μm, the slow shear mode in TeO_2 can be used. It possesses a large M_2, and the slow acoustic phase velocity results in a large τ. Operating frequencies are typically 50 to 100 MHz with bandwidths of 30 to 50 MHz. Transducer dimensions of 4 mm (L) × 1 mm (H) are typical. For f_0 of 60 MHz, the radiation resistance is (assuming a shear $LiNbO_3$ transducer) $\hat{R}_a \approx 400\ \Omega$. We obtain this value under the assumption that the transducer has been matched to the substrate with an *acoustic* quarter-wavelength transformer (see Chapter 6). In an isotropic interaction, the Bragg bandwidth would be only 10 MHz (because of the extremely low acoustic velocity), and the device would be *Bragg limited.* Fortunately, there is a birefringent interaction (because TeO_2 is optically anisotropic) in which a significant improvement in the Bragg bandwidth is possible.

8.5.2 Modulators

In an A/O modulator, the object is to impress the RF signal onto the defracted laser beam. These devices usually require high efficiency and large bandwidth, but only moderate time apertures. Crystals with large indices and high velocities (large M_1) are well suited to this application. Examples include GaP at 630 nm, GaAs at 1.06 μm and Ge at 3.39 μm.

Bandwidths greater than 1 GHz with deflection efficiencies greater than 50% have been achieved. Because the operating frequencies are typically quite high, these devices are usually Bragg limited. To increase the Bragg bandwidth, we usually decrease the transducer height as much as possible. Other techniques to increase the Bragg bandwidth, such as phased arrays, birefringent phase matching, and multiple transducers, will be discussed later.

8.5.3 Acousto-Optic Spectrum Analysis and Signal Processing

The ability of the A/O interaction to deflect discrete acoustic frequencies into discrete optic beams at well-defined angles can be used to spatially transform an RF signal into its component frequencies. Such devices, called *channelizers* because they *channel* the various frequency components, are used in EW and ELINT (electronic intelligence). In the EW application, the channelizer is usually airborne. The requirements are small size, wide bandwidth, and high diffraction efficiency with only low to moderate time aperture. The moderate time aperture is a consequence of the resolution requirement, which is only 1 to 10 MHz, because the devices are designed to intercept radar signals of less than 100 ns duration. Such pulses cannot be resolved any finer than about 10 MHz, and thus the time aperture is typically 100 ns (or an interaction length of 2 to 3 mm). Because the EW channelizer is airborne, it usually requires a solid-state laser diode operating at 830 nm. The longer-wavelength optic beam reduces device efficiency and bandwidth.

The ELINT applications are usually ground based and require moderate to wide bandwidths, high efficiency, and very high time apertures. The large τ results from the requirement that the intercepted signal must be decomposed into its constituent frequencies with a very high resolution. Because size and weight are not at a premium HeNe or Ar ion lasers are usually used, which allow for higher efficiency and bandwidth than does the EW application. Additionally, the low acoustic velocity required for the large τ further increases deflection efficiency. Unfortunately, the time aperture cannot be varied by changing the optical wavelength because D (Figure 8.3) is limited by the time aperture of the device. We can increase τ only by finding a lower velocity cut or by increasing the length of the crystal.

In both applications, the critical factor is the ability of the device to deflect two simultaneous signals (with different frequencies with power levels that can differ by up to 50 dB. This requirement forces the total deflected light to be less than about 3%. We can see this qualitatively from the following argument. Suppose that a strong (RF) pulse is impressed

upon the device and deflects a large percentage of the incident light. If a weak signal is intercepted during this time, it will not be deflected at all, and thus the simultaneous signal capability will be destroyed. Even though the total deflected light power is small, the deflection efficiency (the amount of deflected light per watt of RF power) must be high to reduce nonlinear acoustic effects as well as to reduce the RF drive power of the amplifiers (which may be quite high even if the deflected optic intensity is small). Nonlinearities, caused by either high RF input power or large acoustic power densities, cause spurious acoustic waves, which in turn cause "false alarms" at the photodetector output.

The following are typical of the best results that have been attained. For the wideband channelizer:

1. Gallium phosphide: ⟨1, 1, 1⟩ longitudinal mode with 500-MHz bandwidth centered at 1 GHz and an efficiency of nearly 100% W at 830 nm. Note that there is nothing unphysical about efficiencies greater than 100%/W because they are measured at low diffracted light intensity (in the linear region).
2. Lithium niobate: ⟨0, .809, .588⟩ shear wave (x-polarized) with a 1-GHz bandwidth centered at 2.3 GHz and efficiency of 10%/W at 830 nm.

For the high resolution channelizer:

Slow shear mode ⟨1, 1, 0⟩ with TeO_2 with HeNe laser (630 nm) with a 50-MHz bandwidth centered at 70 MHz and a time aperture of 100 μs (6.2 cm) corresponding to a resolution of 10 kHz.

Wideband and high resolution spectrum analysis are examples of the broader class of A/O signal processing applications. Other examples are adaptive filtering, space and time integrating correlation, ambiguity function computation, and optical matrix multiplication. Adaptive filtering, for example, utilizes the Fourier transform property of the Bragg cell. Because the frequency content of a complex signal appears as a finite array of diffracted light beams, it can be manipulated in real time by passing the beams through addressable pixel elements, which turn on or off individual beams by changing their light transmission properties. This application places very high demands on device acoustic bandwidth because, ideally, the overall bandwidth will adapt to different requirements.

Other applications are generally characterized by complex structures using multiple Bragg cells. System performance depends largely on the time-bandwidth product of the individual Bragg cells, so the overall requirement is similar to that of high resolution spectrum analysis. Because the diffracted light from one device is used as the *incident* beam for a second device, these system architectures place very high demands on

device performance in all three categories of resolution, bandwidth, and efficiency. Like high resolution spectrum analysis, these architectures are usually ground based, realized on large stable optical benches, and utilize sophisticated optical designs. Two exceptions are the surface acoustic wave correlator and the airborne photorecorder. In the former system, the complex optics have been packaged into a "mini" bench by using a small HeNe laser. In the latter system, which employs an Ar ion laser, a massive structure consisting of laser, optics, and mechanical assemblies, is placed on a specially equipped airplane and used to map a section of terrain from high altitudes.

8.6 PERFORMANCE ENHANCEMENTS

8.6.1 Birefringent Acousto-Optic Interaction

As discussed in Chapter 7, when the perturbed index ellipsoid contains a "cross" term, there is a polarization flip (the diffracted beam is orthogonal to the undiffracted beam). If the crystal interaction is such that the two beams "see" different indices of refraction, then the incident and diffracted angles are given by (7.107) and (7.108). At the critical frequency f_s', the *input* angle is stationary while the output angle varies linearly with frequency. Thus, near f_s' the acoustic beam can be well-collimated and still produce a linear variation in output angle with input frequency. The transducer length L can be significantly increased. From Figure 7.9, it is clear that the input curve is approximately parabolic around f_s', so there are limits to the increase in L. Furthermore, the parabolic nature of the input angle results in a deflection efficiency curve as shown in Figure 8.4. The dip in the center reflects the characteristic behavior of the angular deviation for the birefringent interaction, which is determined not between the minimum and maximum frequencies, as in the isotropic interaction, but between *either* the minimum or maximum (which in this interaction are approximately equal) and the critical frequency.

As mentioned previously, f_s' is fixed by the laser wavelength acoustic velocities and indices of refraction, according to (7.111). This severely complicates device design. Further, it is clear that use of the performance advantage inherent in the birefringent interaction requires a geometry with a reasonably high photoelastic constant. It is quite difficult to find a configuration with a critical frequency in a useful band *and* a high photoelastic constant. One geometry that has both is shown in Figure 8.5. We will calculate the effective photoelastic constant for this geometry in Chapter 9. The acoustic mode is the pure shear mode polarized along $\langle x \rangle$. At 633

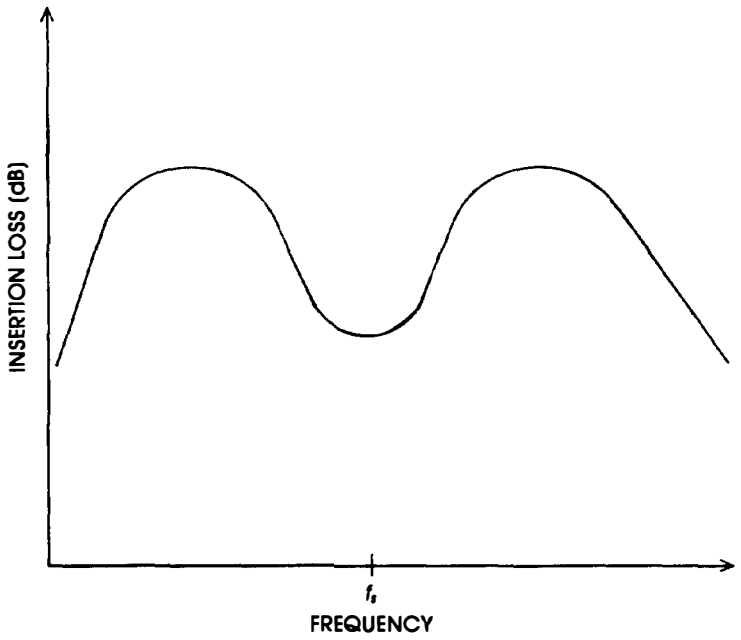

Figure 8.4 Relative diffracted light intensity for a birefringent interaction. The double-hump behavior is a consequence of the parabolic nature of the incident Bragg angle (Figure 7.9).

nm, the indices of refraction are $n_o = 2.29$ and $n_e = 2.2$. At the angle of incidence ($-54°$ from the y- to the z-axis), the extraordinary index is, by (7.24); $n_e' = 2.23$. The acoustic velocity of the pure shear mode is found from the Christoffel equation:

$$v_a = 3.57 \times 10^3 \text{ m/s}$$

Finally, the critical frequency is (from (7.111))

$$f_s' = \frac{v_a}{\lambda_0}\sqrt{n_o^2 - n_e'^2} = 2.85 \text{ GHz}$$

Because $LiNbO_3$ is dispersive, the indices vary with optical wavelength. At 830 nm, they are $n_o = 2.25$ and $n_e = 2.17$. The birefringence is lower at the higher wavelength. At $-54°$, the extraordinary index at 830 nm is $n_e' = 2.197$, and the critical frequency has been reduced to 2.04 GHz. The reduction in f_s' is due both to the decreased birefringence and

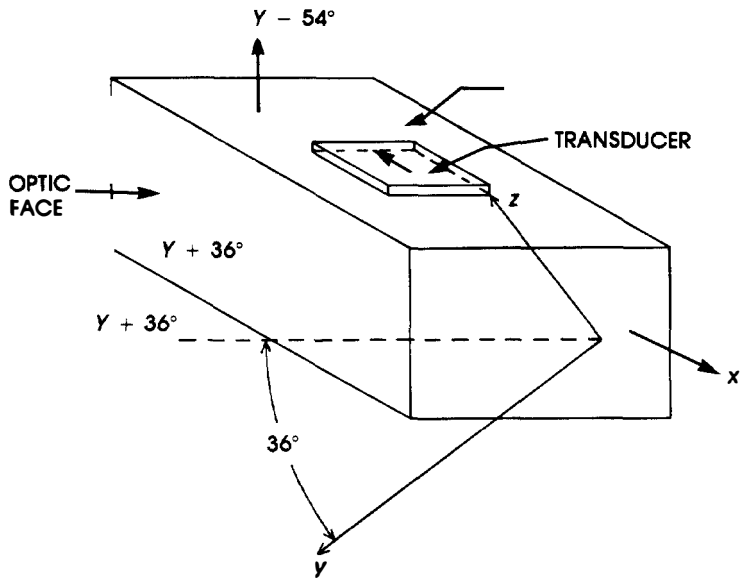

Figure 8.5 Interaction geometry of an important birefringent interaction geometry in lithium niobate. We will investigate this interaction further in Chapter 9.

the increased optic wavelength. The former effect contributes about 6% to the reduction.

Zehl et al. have shown that (7.111) does not accurately predict the critical frequency, because the extraordinary index varies with angle (7.111) assumes a constant value for n_e) [13]. An iterative calculation is required, which yields two critical frequencies for each acoustic mode. These two frequencies correspond to upshifted and downshifted optical modes and thus depend on the angle of the incident optic beam. Thus, for the same device we have the possibility of choosing two critical frequencies, depending on the orientation of the crystal relative to the incident beam. In the previous example, the two critical frequencies are 2.4 and 3.3 GHz at .633 μm and at .83 μm, each frequency is reduced by about 23%, corresponding to the reduced birefringence and increased optic wavelength.

Example 8.3. Find the transducer length L for a 2-GHz Bragg cell centered at 3 GHz operating at 633 nm.

We use the $-54°$ (*y*) device design, so $v_a = 3.6 \times 10^3$ m/s. We choose the upshifted configuration centered close to 3 GHz. Figure 8.6 shows the incident angle as a function of frequency. This figure is identical to Figure

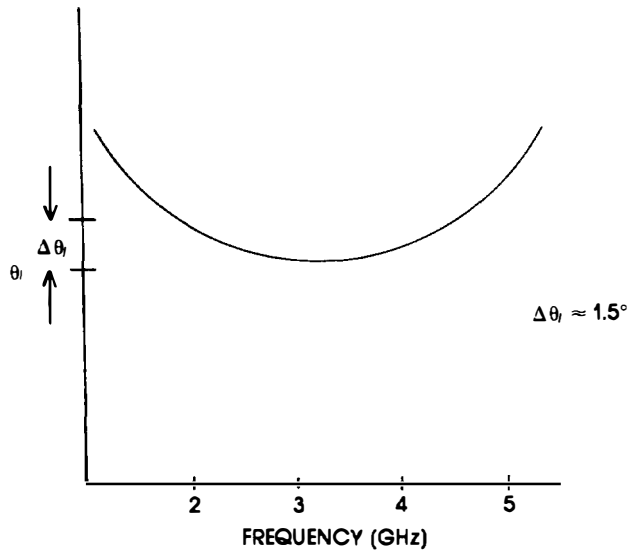

Figure 8.6 Detail of the variation of the incident Bragg angle for a birefringent interaction near the critical frequency. Determining $\Delta\theta_i$ allows us to calculate the transducer length. *Note*: $f_y' = 3$ GHz.

7.9, but has the axes expanded to emphasize that the incident Bragg angle is only stationary over a relatively small band of frequencies. As the acoustic frequency is either increased or decreased from f_s', the incident Bragg angle increases. This variation in angle requires that the acoustic beam spread by an equivalent amount. From the figure, we can see that the angular deviation between the critical frequency and the maximum and minimum frequencies is approximately 1.5°. Thus, the required acoustic diffraction angle is likewise 1.5°, and the transducer length is given by (8.6):

$$d\theta = \frac{v_a}{Lf_s'} = 1.5° = 2.6 \times 10^{-2} \text{ rad}$$

Solving for L, we find the required transfer length = 45μm. This is about the same length required for an isotropic design, with the same center frequency and bandwidth but with $\langle x \rangle$ longitudinal mode in an isotropic interaction (see Example 7.4). It seems that there is thus no particular advantage to the birefringent interaction, but we must not forget that the

velocity of the shear mode is about half that of the longitudinal $\langle x \rangle$ mode, which gives a significant advantage in deflection efficiency. Due to the shape of θ_i *versus* frequency curve near f_s' and the acoustic spreading, a transducer of 45μm will diffract light at the lower, upper, and critical frequencies at approximately equal efficiencies. If the length is increased, the intensity at f_s' will decrease, resulting in the characteristic dip in the efficiency curve, similar to Figure 8.4, because the acoustic spread will be less than the required 1.5°. A transducer length of 90μm, for example, results in a dip of about 3 dB, which is usually acceptable for most applications. This gives an added performance advantage of about 2. In addition, the fact that the acoustic wave is a shear mode implies that the diffracted beam is "flipped" relative to the undiffracted, zero-order beam. With a high-quality polarizer, the zero-order beam can be almost completely eliminated from the photodetector array. Using this scheme reduces the possibility of false alarms and increases the system dynamic range by as much as 10 dB. We show in Chapter 9 that the photoelastic constant for the birefringent interaction is about 70% of the isotropic $\langle x \rangle$. The performance advantage in efficiency comes almost entirely from the ratio of the velocities:

$$\left(\frac{(v_a)_{\text{iso}}}{(v_a)_{\text{aniso}}}\right)^3 = \left(\frac{6.57}{3.57}\right)^3 = 6.2$$

The net performance advantage is about 8. An added advantage of this structure is the higher resolution due to the lower velocity. Because the device is used in EW applications as a wideband spectrum analyzer, the increased resolution is not insignificant.

Fabrication and system integration of this device are quite challenging. Because the transducer length is less than 4 mils, we are forced to choose $L/H = 1$ (we do not realize the performance advantage of $L/H > 1$). The active area is then 8×10^{-9} m^2, which limits the power to less than about $\frac{1}{4}$ W. Wire bonding to such a small area is quite difficult. The optic beam must be focused to 4 mils as it enters the device (which is especially challenging when laser diodes are used). Finally, mechanical and thermal stability must be maintained for the optic and acoustic beams in a variety of environments.

8.6.2 Design of a Birefringent Gallium Phosphide Bragg Cell

We saw in Chapter 7 that a birefringence can be *induced* in an isotropic substrate by the presence of an external stress or an electric field.

We calculated the birefringence for GaAs for a stress applied along one of the principal axes. A possible device configuration using this concept is shown in Figure 8.7. For a force of 78 kg acting over an area of 2.5 $\times$ 10^{-5} m, we showed that the birefringence is $|n_o - n_e| = .001$. Using this value, we find the critical frequency at 633 nm to be $f_s' = 530$ MHz.

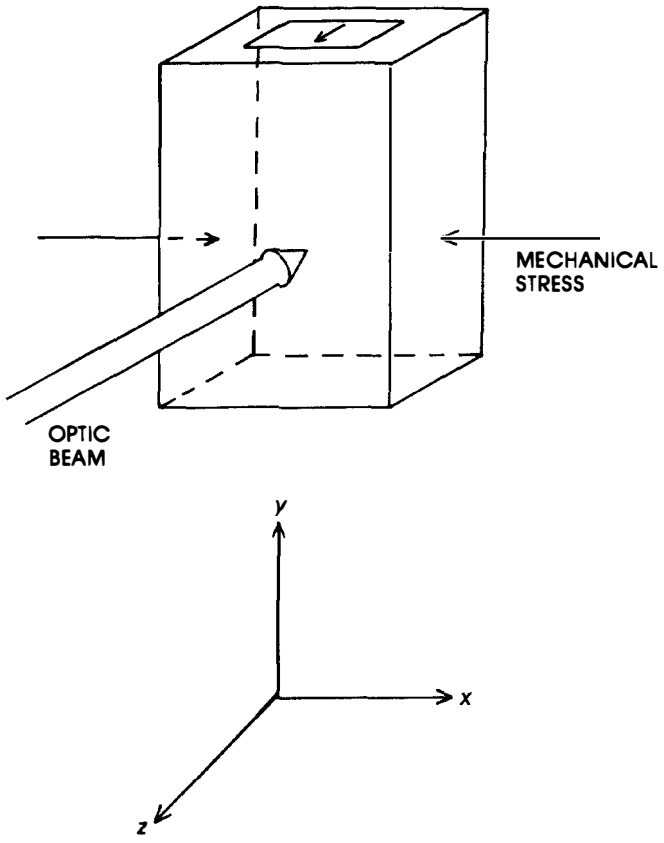

Figure 8.7 Possible configuration for a birefringent A/O interaction in cubic symmetry by using external stress to *induce* a birefringence.

Devices using this concept have been realized with GaP and have been reported [11]. A critical frequency of 300 MHz has been achieved. Because the piezo-optic components do not vary dramatically, pressures greater than 2000 lb/in^2 are required in GaP to produce critical frequencies above 100 MHz. A significant advantage of this structure is that the critical

frequency can be changed in real time. The acoustic bandwidth will not be affected by the optical birefringence and will ultimately limit the total bandwidth unless the critical frequency can be significantly raised. This is due to the fact that the most important advantage of the birefringent design is realized only above 1 GHz where the Bragg bandwidth of the isotropic interaction is reduced by the collimated acoustic beam. The relatively low critical frequency with induced birefringence, even when the crystal is subjected to very large stresses, limits the application of this approach. It is possible, although not likely, that materials will be identified that will permit higher critical frequencies for a given stress.

It is also possible to design an A/O device with an isotropic substrate and an induced birefringent by using the electro-optic effect. The geometry is shown in Figure 8.8. The incident polarization is rotated 45° to correspond to one of the eigenmodes of the crystal. Notice that in the configuration the optic beam enters the device through the electrodes, due to the symmetry of the electro-optic matrix. Optically transparent electrodes, such as indium tin oxide are required. We must be careful to rotate the incident beam so that it corresponds to the faster of the two modes. As in Example 7.1, the two eigenmodes will always be at 45° to the x-axis. The birefringence (and therefore the critical frequency) will depend linearly on the voltage V. Unfortunately, like the stress-induced birefringence, it is not difficult to show that a very large electric field is required to produce even a modest birefringence, at least in GaP.

8.6.3 Birefringent Interaction in Paratellurite

Consider the geometry of Figure 8.9. The slow shear mode polarized $\langle -1, 1, 0\rangle$ propagates in the $\langle 1, 1, 0\rangle$ direction with a phase velocity of 617 m/s. The optic beam is an ordinary mode incident in the $\langle -1, 1, 0\rangle$ direction and polarized in $\langle 0, 0, 1\rangle$. At 633 nm, the indices of refraction for TeO_2 are $n_o = 2.412$ and $n_e = 2.26$. Using (7.111), we obtain the critical frequency $f_s' = 826$ MHz. The high f_s' in this case is due entirely to the large birefringence, because the optic polarization "flips" between the z-axis, where it is a maximum and $\langle 1, 1, 0\rangle$ (in the xy plane), where it is a minimum. Unfortunately, this value of f_s' is unrealistically high, because the slow shear mode cannot propagate above approximately 100 MHz. Furthermore, we will show in Chapter 9 that this interaction is not allowed because of the symmetry of the photoelastic matrix. If the optic beam is now incident along the z-axis (the optic axis), there can be no polarization flipped interaction at all because the ordinary and extraordinary indices of refraction are equal. Intermediate to these two directions, however, the polarization flipped interaction will be birefringent because the two or-

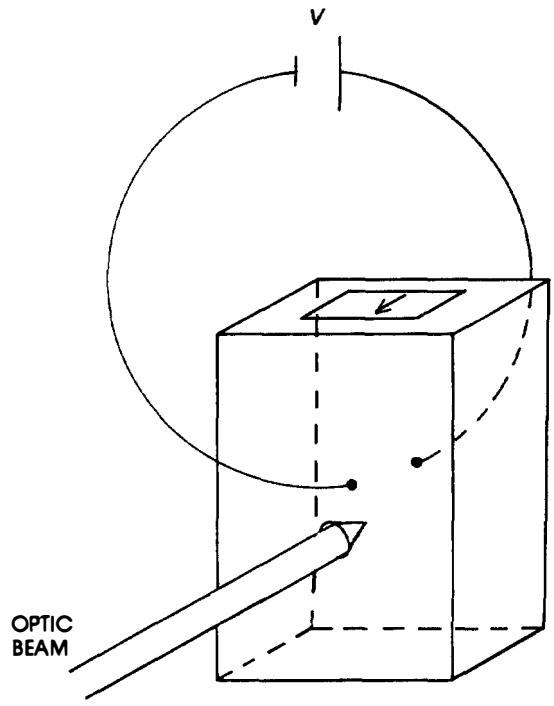

Figure 8.8 Configuration of birefringent interaction in cubic symmetry with induced birefringence by using electro-optic effect. The voltage must be applied to the optic faces (see Example 7.1).

thogonally polarized modes will indeed have different indices (the extraordinary index will be given by (7.24). It is not difficult to show that if the incident optic beam makes an angle of approximately 4° with the z-axis, then the critical frequency will be about 80 MHz.

Paratellurite belongs to a class of crystals known to be "optically active." If a linearly polarized optic beam is incident along the z-axis, the direction of polarization rotates through an angle that depends on the optical path length in the crystal. This phenomenon occurs in a number of optic and acoustic crystals, the most important example being crystal quartz. It cannot be described by straightforward application of symmetry properties. Further, it can occur in optically isotropic materials. We say that the crystal possesses *rotatory power*. As a result of the optical activity in TeO_2 the z-axis is not an optic axis. In acoustic terms, the shear degeneracy along the z-axis is broken in the optic slowness curves.

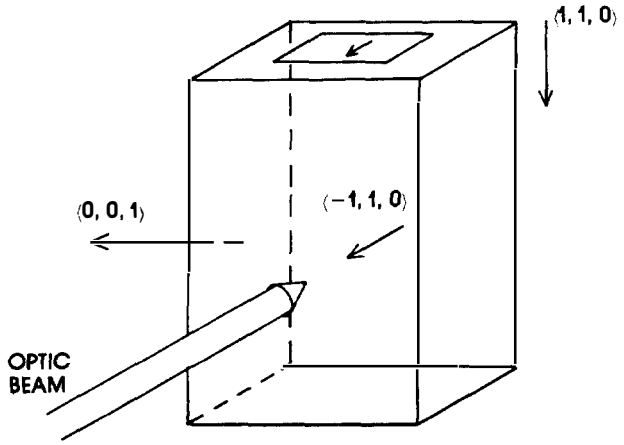

Figure 8.9 Possible configuration for birefringent interaction in TeO_2 by using the "slow" shear mode.

Similarly to a birefringent medium, there are two eigenmodes. In an optically active crystal, they consist of *circularly* polarized modes. Thus, if a right (or left) circularly polarized optic beam is incident on the z-axis, it will propagate unchanged through the body of the crystal. If the mode undergoes an A/O interaction with the ⟨1, 1, 0⟩ propagating slow shear wave, it will be "flipped" into the circularly polarized mode of the opposite sense (i.e., the right circularly polarized mode will flip to the left mode, or *vice versa*). Because these two modes propagate with different phase velocities, the interaction is birefringent and possesses a critical frequency that, like the more conventional birefringence, depends on the optic wavelength. This case has been analyzed by Warner *et al.*, who show that the birefringence corresponds to a critical frequency of approximately 80 MHz at 633 nm, making this mode of operation quite useful.

8.6.4 Use of Acoustic Anisotropy

As we have seen, cubic crystals become birefringent only under the application of an external stress or electric field. They are, however, naturally anisotropic acoustically. As shown in Chapter 3, the anisotropy is geometrically represented by the curvature of the slowness curve. For example, only the pure shear mode in the principal planes is isotropic, because its slowness curve is circular. The shape of the slowness curve near a symmetry axis can be described by a power series expansion as in

(3.16). We showed that it is possible to find (usually for shear modes) propagation directions for which the value of b (in (3.16)) is greater than or equal to $\frac{1}{2}$, so either focusing or self-collimation of the acoustic beam occurs.

Hecht and Petrie have used this concept to determine a crystal orientation in GaP in which the acoustic beam is self-collimating. The required acoustic direction is $\langle 1, -1, 0 \rangle$. The interaction geometry is shown in Figure 8.10. An optic beam incident along the $\langle 1, 1, -2 \rangle$ direction encounters an acoustic beamwidth that does not spread (reducing the Bragg bandwidth dramatically). If, however, the beam is incident perpendicular to this direction, in the $\langle 1, 1, 1 \rangle$ direction the diffraction *loss* (due to finite transducer height H) is dramatically reduced. Unlike optical anisotropy, in which transducer length can be increased over the value given by (8.8) without adversely affecting the Bragg bandwidth, acoustic anisotropy allows a reduction in transducer *height* H that results in improvements in deflection efficiency and resolution. The reduction in H is limited only by the difficulty in wire bonding and focusing the optic beam to a very thin transducer. Unfortunately, the reduction in H is at the expense of a similar reduction in the photoelastic constant, which we will show in Chapter 9.

8.6.5 Acoustic Phase Arrays

Use of optical and acoustic anisotropies depends on the material properties of the crystals. Neither phenomenon has been universally incorporated into A/O device designs. In the birefringent interaction, there is always a critical frequency that often is either too high or too low to be useful in practical devices, or else configuration of the interaction corresponds to a photoelastic constant that is quite small. Likewise, as we shall see in Chapter 9, the use of acoustic anisotropy, at least in GaP, results in a photoelastic constant that is less than optimal. An alternative technique involves the use of a series connection of acoustic radiating elements, as described in Chapter 6, in which the *spacing* of the radiators is such that they form an acoustic phase grating. Because this technique does not depend on the acoustic or optic properties of the interaction medium, it can be incorporated into any design regardless of the acoustic or optic propagation directions. The individual elements diffract, and their acoustic interaction causes the direction of the beam to change. If the elements are connected as in Figure 6.20, then the nearest neighbors are π out of phase. The essence of this technique, which is also referred to as *beam steering*, is that the phase grating results in an acoustic beam whose direction varies with frequency in such a way that the acoustic beam remains at or near the Bragg angle over an appreciable frequency band. Like the birefringent

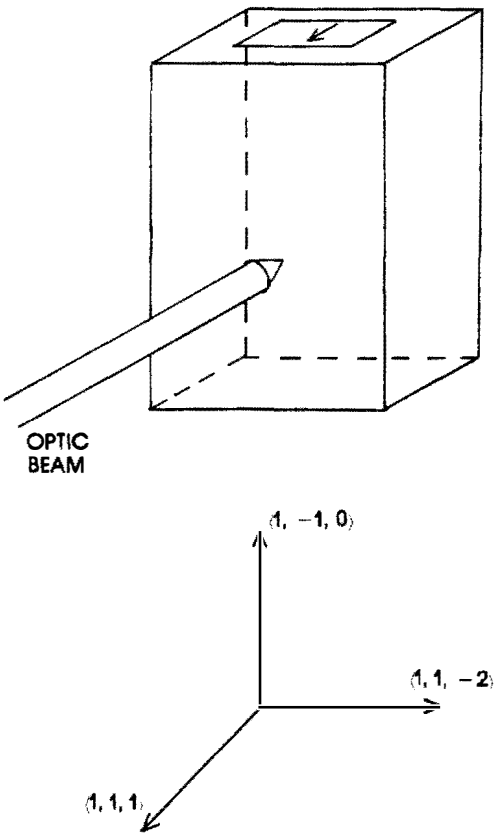

Figure 8.10 Isotropic interaction in GaP by using acoustic anisotropy to collimate the acoustic beam so that there is reduced diffraction spread normal to the optic faces.

interaction, acoustic beam steering allows L to be increased without adversely affecting the bandwidth. The spacing of the elements determines the amount of beam steering, which is the principal design issue in applying the technique. Weinert shows that the optimum element spacing is given by [6]:

$$h = \frac{v_a^2}{\lambda_0 f_s^2 n} \tag{8.18}$$

Like the birefringent interaction, acoustic beam steering requires prior knowledge of the optical wavelength. The most serious problem is the inverse-squared frequency dependence of the element spacing, which allows the technique to be most useful at low frequencies where the Bragg bandwidth is naturally large (and beam steering is not required). At very high frequencies, where it is especially needed, it is quite difficult to fabricate the elements with the required h. For example, in a GaP A/O deflector at 1 GHz (with a longitudinal wave), the required h is only 20 μm at .633-μm optic wavelength. If the spacing is increased, the acoustic beam will steer, but the effectiveness of the technique will be reduced. Nevertheless, increases in efficiency of between 200 to 300% have been reported in GaP devices operating at 1 GHz. Because of the small transducer spacing required at very high frequencies, this technique works best with sputtered film technology in which the phased array may be defined photolithographically.

8.6.6 Multiple Acoustic Beams

Closely allied with the phased array technology is the use of multiple acoustic beams, as shown in Figure 8.11. In this technique, the required frequency band is broken up into two or three sub-bands with one transducer for each band. The individual transducers are oriented at different Bragg angles, depending on the specific frequency range. This allows for optimization in the acoustic as well as the Bragg bandwidths by varying the thickness of each transducer. Like the phased array design, this technique can be incorporated into an isotropic or anisotropic (optically or acoustically) device. Delaney and Yao fabricated a Bragg cell with a bandwidth of 1.3 GHz at .83 μm by using two acoustic beams, with each beam composed of a phased array of transducers [15]. The band was broken up into low and high frequency sub-bands centered at 1.6 GHz and 2.25 GHz. The low band consisted of 30 individual transducers, the high band 48. The fabrication technology used was sputtered ZnO ($\langle z \rangle$−axis) on $\langle x \rangle$ $LiNbO_3$ (longitudinal), and the acoustic arrays were defined by standard photolithographic techniques.

Example 8.4. Design a 1-GHz bandwidth GaP Bragg cell centered at 1.5 GHz, using two transducers. The acoustic wave propagates along $\langle 1, 1, 1 \rangle$ (longitudinal), $v_a = 6.65 \times 10^3$ m/s, and the optic wavelength is .83 μm. For the low band, we choose

$$\begin{aligned} \text{frequency band} &= 1\text{–}1.6 \text{ GHz} \\ \text{BW} &= .6 \text{ GHz} \\ f_0 &= 1.3 \text{ GHz} \end{aligned}$$

Using (8.8), we find $L_1 = 230$ μm. For the high band, we choose

$$\begin{aligned} \text{frequency band} &= 1.6\text{–}2 \text{ GHz} \\ \text{BW} &= .4 \text{ GHz} \\ f_0 &= 1.8 \text{ GHz} \end{aligned}$$

In this band, (8.8) yields $L_2 = 240$ μm. Had the device consisted of a single transducer, the required length would have been 100 μm, so using two transducers has resulted in an increased L and a performance improvement of over 100%. The larger radiating area reduces nonlinear acoustic effects and facilitates fabrication. The angle α relates to the difference in center frequencies between the two beams. For a .5-GHz difference, it is approximately 3°.

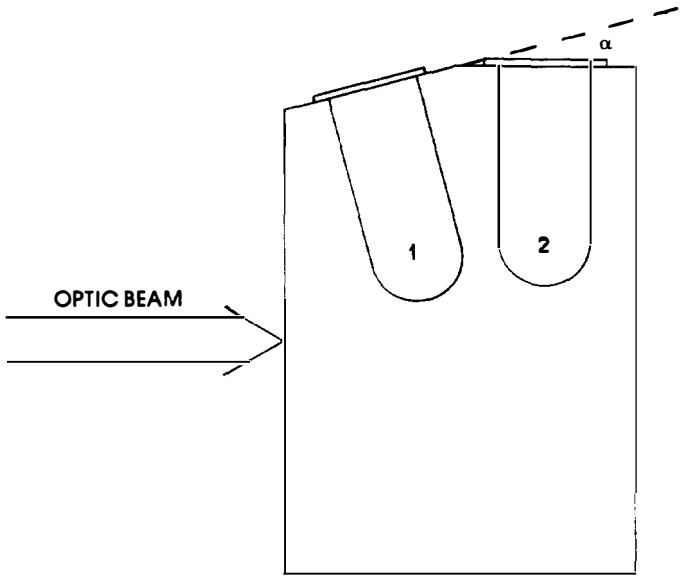

Figure 8.11 Use of multiple acoustic beams to increase the Bragg bandwidth. At low frequencies, depending on the angle of incidence, the interaction with the left wave is more efficient, whereas at higher frequencies the beam interacts with the right acoustic wave.

8.6.7 Multiple Acoustic Beams from a Single Transducer

It is also possible to produce two acoustic beams with different phase velocities radiating from a single transducer. The most straightforward approach is to use a transducer that excites two (orthogonally polarized) shear modes, such as ⟨x⟩ $LiNbO_3$. The disadvantage of this approach is that only one of the modes is strongly excited. An alternative technique is shown in Figure 8.12 [12]. In this geometry, the GaP crystal is oriented such that the acoustic wave propagates along ⟨1, 1, 0⟩. The transducer is ⟨x⟩ shear $LiNbO_3$ (we disregard the weakly excited mode) and is oriented so that in the substrate the polarization is ⟨−1, 1, 1⟩. The eigenmodes of the crystal for this orientation are ⟨0, 0, 1⟩ and ⟨−1, 1, 0⟩, and they are not degenerate. Thus, both of these modes are excited. The ⟨0, 0, 1⟩ is the fast shear mode and propagates with $v_a = 4.13 \times 10^3$ m/s, while the slow shear mode propagates with $v_a = 3.08 \times 10^3$ m/s. Each of these modes interacts independently with the optic beam, which is incident along ⟨−1, 1, 1⟩. At a given frequency, the fast shear mode has a longer acoustic wavelength and thus a smaller Bragg angle. The interaction is more efficient at lower frequencies with the slow shear wave and more efficient at higher frequencies with the fast shear wave. The increase in Bragg bandwidth is approximately equal to the ratio of phase velocities (in this case 1.3).

8.6.8 Use of New Materials

Generally, crystals with low attenuation, high index of refraction, and moderate to high velocities are optimal for wideband applications, whereas high resolution devices require low velocity and low attenuation. High optical quality, hardness above 4 (on the mho scale), ease of handling, and mature growth techniques are secondary but desirable properties. To date, GaP and $LiNbO_3$ fill the requirements best for wideband devices, and TeO_2 is used when high τ is required. Increased system performance constantly drives the search for better materials, however.

Three promising candidates are thallium arsenic sulfide (Tl_3AsS_4) and GaAs for wideband applications, and mercurous chloride (Hg_2Cl_2) for high resolution applications. Like GaP, Tl_3AsS has a very high index of refraction and is transparent well into the visible region [14]. Its longitudinal velocity (for z-cut) is about one third that of GaP, which causes a reduced Bragg bandwidth but increased efficiency by a factor of over 20. Attenuation is moderate (about an order greater than GaP), in keeping with its lower velocity. The frequency dependence is far from f^2 (due to

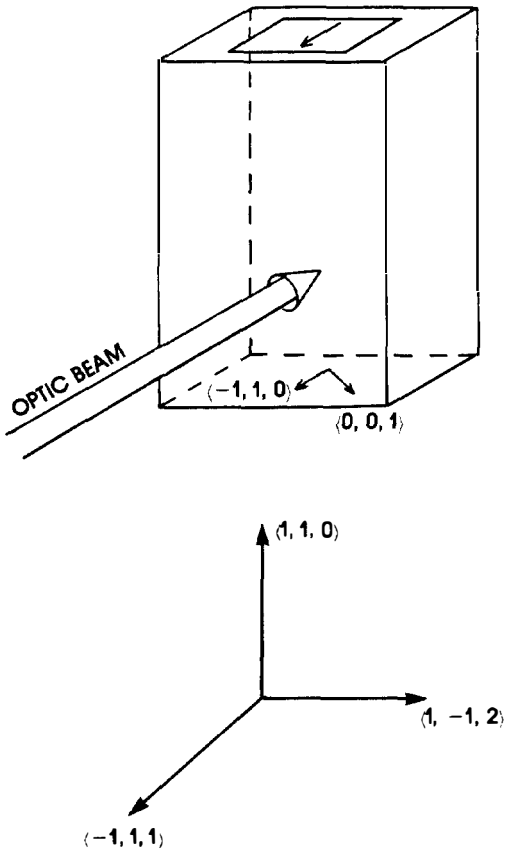

Figure 8.12 Use of multiple acoustic beams from a single transducer. The *acoustic* polarization direction of the transducer does not belong to an eigenmode of the substrate.

relatively immature growth techniques), which suggests that further improvements are likely. It should be an optimal material in the frequency range of 200 MHz to 1 GHz.

Gallium arsenide is quite similar to GaP in most of its acoustic and optical properties. It has a very high index, which results in an increase in diffraction efficiency over GaP by a factor of about 4, but does not transmit below about 1 μm. Its relatively low attenuation would indicate

applications in the gigahertz range using optical wavelengths above 1 μm possibly in fiber optic applications.

Mercurous chloride, like TeO_2, has an anomalously slow shear mode in ⟨1, 1, 0⟩ [10]. Its velocity is about half that of TeO_2, it transmits in the visible region, and its attenuation is not horrendously large. It is thus an ideal candidate for very high resolution applications.

Example 8.5. Design of a Thallium Arsenic Sulfide Bragg Cell [14]: Thallium arsenic sulfide (Tl_3AsS_4) is characterized by very low acoustic velocities and moderate attenuation. It is thus an optimal crystal for devices in the .2–1 GHz frequency range. It has orthorhombic symmetry, and thus the velocity curves in the three principle planes have the form of Figures 3.9 to 3.11. There are no shear degeneracies along the principle axes, and propagation along ⟨1, 1, 0⟩ does not result in an anomalously slow shear velocity. Tl_3AsS_4 is optically biaxial, and thus has three indices of refraction. Neither of the optic axes coincides with the z-axis. At .633 μm the incides are

$$n_1 = 2.829, \quad n_2 = 2.774, \quad n_3 = 2.825$$

In Tl_3AsS_4 there are isotropic A/O interactions, which involve the longitudinal acoustic modes. In one such design a peak efficiency of over 400% RF watt has been achieved. There are also birefringent, polarization flipped interactions, which utilize shear modes. The existence of three indices complicates device design, but also increases design flexibility. Notice, for example, that the birefringence in the x-y plane ($n_1 - n_2$) is much larger than in the x-z plane ($n_1 - n_3$). For an acoustic shear mode propagating along the x-axis and polarized along y, interacting with an optic beam incident along z, the polarization flip is between x and y. This high birefringence operation uses the slow shear mode with velocity $.6 \times 10^3$ m/s, and thus has a critical frequency (from (7.111)) of about 550 MHz. If the x propagating shear wave is polarized along z and the optic incidence is along y, the polarization flip is between x and z. This low birefringence mode uses the fast shear mode ($v_a = 1.2 \times 10^3$ m/s), corresponding to a critical frequency of approximately 300 MHz at .63 μm. Even in this relatively simple case of acoustic propagation along a single axis, device design can be quite complex. In the next chapter, we investigate techniques for dealing with acousto-optic interactions for general acoustic and optic propagation directions.

PROBLEMS

8.1 Calculate the radiation resistance of the Bragg cell of Example 8.3, assuming that $L/H = 1$. Locate the impedance characteristic on the Smith chart and suggest possible matching techniques.

8.2 Design a birefringent $LiNbO_3$ Bragg cell using the $-54°$ $\langle y \rangle$ configuration operating at a center frequency of approximately 2.5 GHz with a 1-GHz bandwidth. Suggest a reasonable value for L/H and discuss RF matching.

8.3 Find the required transducer length L for the $\langle x \rangle$ longitudinal (isotropic) interaction ($v_a = 6.6 \times 10^3$ m/s) in $LiNbO_3$ centered at 2.5 GHz with a 1-GHz bandwidth and compare the performance with the results of Example 8.2.

8.4 Estimate the performance advantage gained by employing a birefringent GaP device with critical frequency of 500 MHz over the isotropic design at the same frequency. Make reasonable assumptions about the bandwidth, L/H and radiation resistance.

8.5 Calculate the voltage required to produce a birefringence of .1% in GaP in the geometry shown in Figure 8.8.

8.6 Design a 1-GHz bandwidth Bragg cell using three transducers operating at a center frequency of 2 GHz. Make reasonable assumptions about the sub-band frequencies and estimate the performance advantage gained over using a single transducer.

8.7 Discuss the bandwidth of a Tl_3AsS_4 Bragg cell operating in the low birefringence mode (Example 8.5). What is a reasonable value for the transducer length L. Consider both Bragg and acoustic bandwidths. Under what conditions is such a device Bragg-limited?

8.8 Repeat Problem 8.7 for the high birefringence mode.

8.9 Show that the critical frequency f_s' for the birefringent interaction in TeO_2 is 80 MHz, if the optic incidence is 4° from the z (optic) axis.

REFERENCES

1. N. Berg and J. Lee, eds., *Acousto-Optic Signal Processing,* Marcel Dekker, New York, 1985.

2. D. Hecht, "Broadband Acousto-Optic Spectrum Analysis," *Proc. IEEE Ultrasonics Symposium,* 98 (no date).
3. A. Yariv and P. Yeh, *Optical Waves in Crystals,* John Wiley and Sons, New York, 1984, Chapters 7 to 9.
4. J. Bagshaw and T. Willats, "Anisotropic Bragg Cells," *GEC Journal Res.* **2,** 96 (1984).
5. E. Gordon, "A Review of Acoustooptical Deflection and Modulation Devices," *Proc. IEEE*, **52** (10), 1391 (1966).
6. R. Weinert, "Very High-Frequency Piezoelectric Transducers," *IEEE Trans. Sonics Ultrasonics* **SU-24,** 48 (1977).
7. A. Warner, D. White, and W. Bonner, "Acousto-optic Light Deflectors Using Optical Activity in Paratellurite," *J. Appl. Phys.* **43** (11), 4489 (1972).
8. T. Yano and A. Watanabe, "Acousto-optic Figure of Merit of TeO_2 for Circularly Polarized Light," *J. Appl. Phys.* **45** (3), 1243 (1974).
9. D. Hecht and G. Petrie, "Acousto-optic Diffraction From Acoustic Anisotropic Shear Modes in Gallium Phosphide," *Proc. 1980 IEEE Ultrasonics Symposium,* 474 (1980).
10. M. Gottlieb, A. Goutzoulis, and N. Singh, "Mercurous Chloride Acousto-optic Devices," *Proc. 1986 IEEE Ultrasonics Symposium,* 423 (1986).
11. Z. Azamotov, V. Voloshinov, F. Mamatdzhanov, and V. Parygin, "Anisotropic Diffraction of Light in a Gallium Phosphide Crystal with Induced Anisotropy," *Sov. J. Quantum Electron.* **11** (9), 1232 (1981).
12. J. Soos, R. Rosemeier, and J. Rosenbaum, "Optimization of Shear Modes to Produce Enhanced Bandwidth in GHz Gap Bragg Cells," *Proc. SPIE.*
13. O. Zehl, R. Bonney, M. Price, and J. Rosenbaum, "Features of Birefringent Diffraction in Wideband Bragg Cells," *Applied Optics,* **24** (4), 448 (1985).
14. A. Goutzoulis, *et al.*, "Thallium Arsenic Sulfide Acousto-Optic Bragg Cells," *Applied Optics,* **24** (23), 4183 (1985).
15. M. Delaney and S. Yao, "Wideband Acousto-Optic Bragg Cell," *Proc. 1982 IEEE Ultrasonics Symposium*, 408 (1982).